PHYSICAL REVIEW B VOLUME 33, NUMBER 4 15 FEBRUARY 1986

Thermoreflectance studies of transition-metal dichalcogenides between 1 and 9 eV

A. Borghesi, Chen Chen-jia,* G. Guizzetti, L. Nosenzo, E. Reguzzoni, and A. Stella
Dipartimento di Fisica "A. Volta" dell'Università, 27100 Pavia, Italy

F. Lévy
Institut de Physique Appliquée, Ecole Polytechnique Fédérale, Lausanne, Switzerland

(Received 24 July 1985)

In this work the optical structures due to interband transitions of group-IV transition-metal dichalcogenides have been studied by means of thermoreflectance. The investigated photon energy ranges from 1 to 9 eV, which is a considerable extension with respect to similar previous works. Attention has been focused on the optical properties of the system $Ti_{1-x}Hf_xSe_2$, which changes from semimetallic to semiconducting as a function of composition. In particular, the "anomalous" evolution of the energy positions of optical structures of the interband spectrum versus lattice and other structural parameters as well as composition has been analyzed. Different behavior of two plasma resonances in the interband spectrum as a function of composition has been seen.

I. INTRODUCTION

Transition-metal dichalcogenides (TMD's) have been the object of extensive studies which have yielded a rather comprehensive "picture" of their structural, electrical and optical properties.[1] They are layered compounds of formula TX_2, where T is a transition-metal atom from group-IVA, -VA, or -VIA columns of the Periodic Table and X is a chalcogen atom (S, Se, or Te).

The two-dimensional (2D) X-T-X layers or sandwiches are loosely bound by van der Waals–type forces. Within each sandwich, the transition metal atoms T and the chalcogen atoms X form 2D hexagonal arrays. Two distinct 2D crystal structures are obtained, depending on the relative alignment of the two X-atom planes within a single X-T-X sandwich: the metal atoms are coordinated by six neighboring chalcogen atoms either in an octahedral or a trigonal prismatic configuration, as shown in Fig. 1(a). Several polytypes of a given compound can be formed, according to stacking and the number of the X-T-X sandwiches perpendicular to the c axis in the unit cell (in the notation 1T, 2H, and 3R, the integers represent the number of slabs in the unit cell and T, H, and R denote trigonal, hexagonal, and rhombohedral symmetries, respectively).

In a simplified picture we can draw the electronic energy levels sketched in Fig. 1(b). While the group-VI TMD's (2H-MoS_2,WSe_2,...) are semiconductors with a hybridization gap of the order of 1–2 eV, between the d_{z^2} filled band and the higher empty d bands, group-V TMD's ($NbSe_2$) are metals with a half-filled d_{z^2} band. In group-VI TMD's, excitonic structures have been evidenced and resolved, whereas in group-V TMD's charge-density wave (CDW) phase transitions have shown up as a dominant feature.

Group-IV TMD's represent a somewhat intermediate case, since the generally small separation between empty d bands originating from TM atoms and filled p band originating from chalcogen atoms is responsible for the semiconducting character of these compounds, evolving to a semimetallic behavior when conduction and valence bands partially overlap as in $TiSe_2$. In this case, electrical and optical properties are affected very strongly.

In this paper we concentrate our attention on the

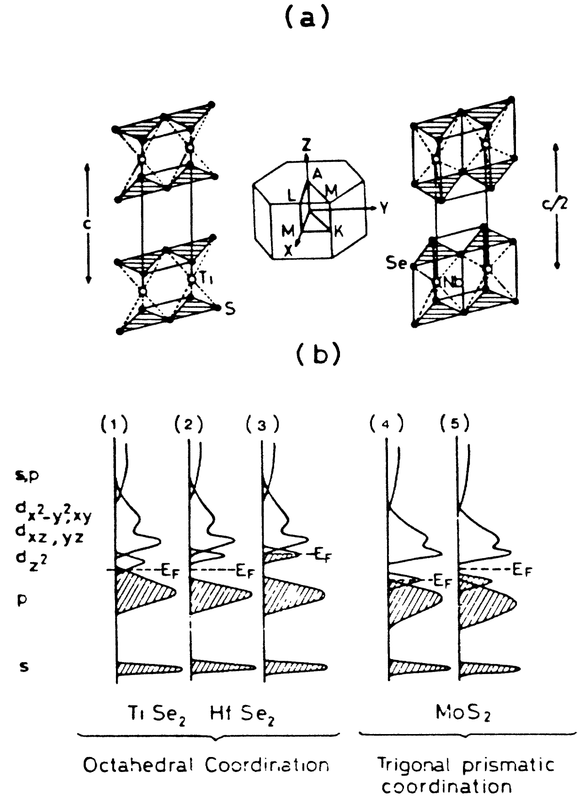

FIG. 1. (a) Brillouin Zone and crystal structures for TMD's, both in the octahedral and trigonal prismatic coordination. (b) Simplified picture of electronic energy level diagram for group-IV TMD's (1) and (2), a group-V TMD (3), and group-VI TMD's (4) and (5).

group-IV TMD's (T=Ti, Zr, Hf and X=S, Se) characterized by an octahedral coordination and D_{3d}^3 ($P\bar{3}m1$) space group. Among the major features of this family of compounds we mention a structural phase transition in the semimetallic $TiSe_2$, leading to the formation of a $2\times2\times2$ superlattice. Such a phase transition can be controlled by varying the stoichiometry as long as the system is semimetallic, but has never been observed in any semiconductor of the series.

The recent literature reports a considerable number of works concerning band calculations of these compounds.[2–16] While agreement is found in the general aspects of the energy level picture, some discrepancies still exist in the finer details, for example, the attribution of the optical gap to transitions at specific high-symmetry points of the Brillouin zone (BZ). Nearly all the compounds of the series have been examined with different approaches, but a unique calculation considering all or most group-IV TMD's is still lacking.

Specific attention has been devoted to the case of TiS_2 and $TiSe_2$. The former is expected to be a semiconductor and its high free-carrier response suggests high degeneracy due to imperfect stoichiometry. For the second one, $TiSe_2$, the semimetallic character has been theoretically investigated[17] in connection with the structural parameter z, which is related to the Ti-Se distance in the formula

$$d=(\tfrac{1}{3}a^2+z^2c^2)^{1/2} . \qquad (1)$$

From the experimental point of view, the general optical properties of group-IV TMD's have been known since 1965 from the pioneering work of Greenaway and Nitsche,[18] who examined the room-temperature reflectivity of several TMD's. Recently, Bayliss and Liang[19] have performed an accurate study of the reflectivity R, between 1 and 4 eV, of most of the TMD's using polarized light parallel and perpendicular to the **c** axis.

The characteristic R spectra, having a great number of weak features superimposed on broad bands, indicate the possibility of applying successfully a derivative spectroscopy technique. Thus, an extensive study of these compounds, by means of the thermoreflectance (TR) technique, was undertaken.

In view of the above reported considerations, in this work we intend: (i) to obtain a detailed classification of the optical spectra of the compounds, with particular attention to their dependence on simple parameters such as bond length or lattice constants; (ii) to do that not only by considering the various combinations of T and X atoms in TX_2 compounds, but also by smoothly driving the mixed compound $Ti_{1-x}Hf_xSe_2$ from semimetal to semiconductor; (iii) to observe the evolution of the optical spectra of mixed crystals also in connection with the behavior of the parameter z and to give a precise picture of "anomalies" and possible bowing effects; (iv) to relate our results to the currently available band calculations.

In Sec. II the experimental apparatus and sample preparation are briefly described, in Secs. III and IV the interband spectra of the pure compounds and of $Ti_{1-x}Hf_xSe_2$, respectively, are reported and in Sec. V the main conclusions are summarized.

II. EXPERIMENTAL DETAILS

The dimensions of the samples used in the present work were about $3\times3\times0.2$ mm^3. The single crystals were grown by iodine chemical transport reaction. The mixed crystals could be grown only in the range $0\leq x\leq0.5$. Shortly before the experiment, they were cleaved or their surfaces were carefully cleaned by rubbing them on a cloth drenched with methyl alcohol.

The experimental apparatus used to measure TR spectra, i.e., determining wavelength-dependent relative variations $\Delta R/R$ of the reflection coefficient R produced by a temperature modulation ΔT, has been discussed in detail in previous papers (see, for example, Refs. 20 and 21).

Here we recall some of the most basic experimental features. Radiation was supplied by a homemade low-pressure hydrogen discharge lamp in the uv-visible region and by a quartz halogen lamp in the ir region, connected with a grating 218 McPherson monochromator. A sodium salicilate—coated R 980 Hamamatsu photomultiplier and a 150 CVP Philips photomultiplier have been used as light detectors in the two regions. The working pressure $p\simeq10^{-8}$ Torr was reached by ionic pump. A temperature modulation $\Delta T\simeq1$ K of the sample was obtained at 1.5 Hz by indirect heating, using a 1-Ω Ge heater fastened to the copper sample holder. The crystals were gently pressed against the heater and a thin layer of vacuum grease ensured a good thermal and mechanical contact. The modulation signal ΔR was detected by means of the conventional lock-in technique and integrated in order to improve the signal-to-noise ratio.

The reflectivity was measured with the same optical apparatus by means of a double-beam, double-photomultiplier optical system. Signal processing was achieved by using two lock-in amplifiers, an analogic ratiometer and a final integrator in order to enhance the sensitivity. The correction of the zero line was made *a posteriori*. The frequency derivative of the reflectivity $dR/d\nu$ was computed from the R data.

III. TR SPECTRA OF THE PURE COMPOUNDS

The R spectra of the pure compounds[18–20] are characterized by the existence of distinct minima, sometimes referred to as "windows," with different relevance for the various crystals of the series. They are generally attributed to the exhaustion of transitions involving specific valence and conduction bands (or subbands), and are indicative of plasma resonances. Superimposed on the broad bands separated by such minima, a number of fine structures appear, due to interband transitions at high-symmetry points of the BZ.

The TR technique gives a different response to these two aspects: interband transitions yield weak features in the TR spectrum, whereas R minima cause strong dispersionlike TR signal. More precisely, as to the latter, it is possible to account for the TR line shape by fitting the gross behavior of the reflectivity through a suitable number of Lorentzian curves, and then by supposing that a temperature-modulated broadening mechanism acts on all of the optical bands. Modulation of the frequency position ν_0 (shift modulation) cannot yield the experimental

TR lineshape. We note that R minima are at the same energies as the Im $\tilde{\epsilon}^{-1}$ peaks, obtained by energy-loss spectroscopy.[22,23] Thus TR spectra results are very effective for indication the existence of collective excitations.

For what concerns the interband transitions, we recall that the signal from an optical structure characterized by energy position ν_0 and broadening parameter Γ, can generally be written as

$$\frac{\Delta R}{R}=\frac{1}{R}\left[\frac{\partial R}{\partial \nu_0}\frac{d\nu_0}{dT}+\frac{\partial R}{\partial \Gamma}\frac{d\Gamma}{dT}\right]\Delta T \ . \qquad (2)$$

The two terms on the right-hand side represent the so-called "shift" and the "broadening" contributions. When shift predominates as modulation mechanism, TR spectra look similar to the first frequency derivative of reflectivity ($dR/d\nu$) and zero crossings (from positive to negative) correspond to peaks in R. If broadening dominates instead, the TR line shape is quite different: in the case of a Lorentzian band,[21] for example, negative minima correspond to peaks in reflectivity, as it appears in Fig. 2, which compares the R and TR curves for the HfS_2 crystal in the energy range 2.5–4 eV. The predominance of broadening has been verified for the TR spectra of all the crystals studied. Typical values of 3×10^{-5} eV/K and of 1.5×10^{-4} eV/K are obtained for the shift ($d\nu_0/dT$) and broadening ($d\Gamma/dT$) thermal coefficient, respectively, of the lower-energy optical structures.

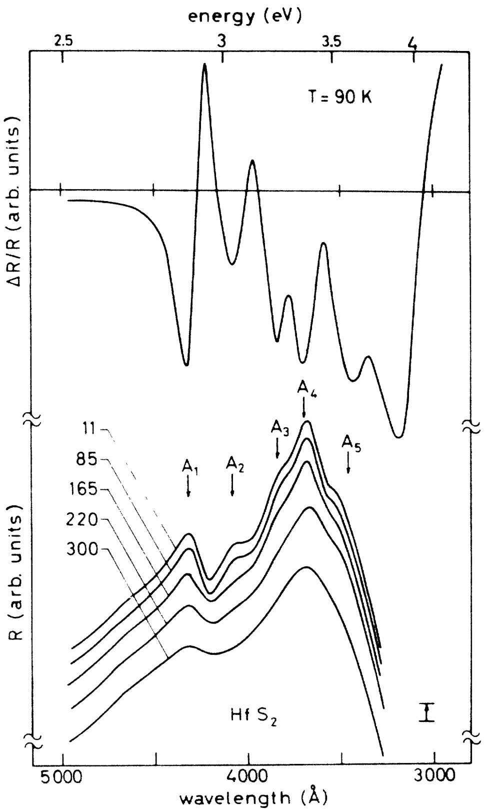

FIG. 2. Thermoreflectance spectrum at 90 K for a HfS_2 crystal, compared with reflectance spectra at different temperatures. For clarity the ordinates of each curve have been displaced as indicated by the arrow.

TABLE I. Lattice parameters a, c, and bond length d for the pure TMD's studied in the present work. The data are taken from the literature (Ref. 8).

	a (Å)	c (Å)	d (Å)
TiS_2	3.40	5.69	2.42
$TiSe_2$	3.54	6.00	2.53
ZrS_2	3.66	5.82	2.57
$ZrSe_2$	3.77	6.14	2.66
HfS_2	3.64	5.84	2.56
$HfSe_2$	3.75	6.16	2.66

Thus we assume that minima in the TR spectrum represent highly reliable energy positions for the optical structures associated with the interband transitions in the investigated system. This enables one to determine with high resolution the energy gaps and more generally the photon energy of the typical structures in the optical spec-

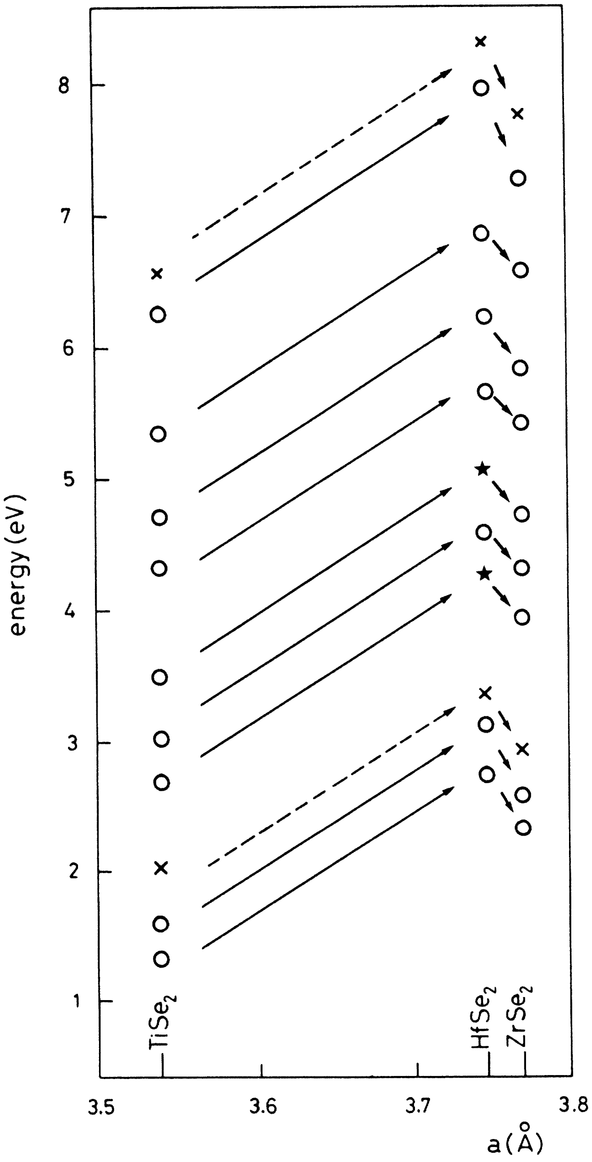

FIG. 3. Energies of optical structures in interband spectrum plotted against lattice parameter a for the sequence $TiSe_2$-$ZrSe_2$-$HfSe_2$.

TABLE II. Energies (expressed in eV) of the structures of TR interband spectra for the group-IV TMD's. Energies labeled with an asterisk are obtained by means of interpolation, as in Fig. 3.

	A_1	A_2	A_3	A_4	A_5	B_1	B_2	B_3	B_4	B_5	B_6	B_7
TiS_2		1.48	1.72	1.85*	2.00	3.32	3.75	4.50*	5.15	5.40*	6.30*	7.05
ZrS_2	2.40	2.59	2.71	2.95	3.25	4.70	5.05	5.58	5.80	6.25	7.20	7.70
HfS_2	2.85	3.04	3.22	3.36	3.60	5.10	5.50	6.10	6.40*	6.80	7.50	7.95
$TiSe_2$				1.34	1.55	2.70	3.00	3.45	4.32	4.72	5.36	6.20
$ZrSe_2$	1.65	1.95	2.75	2.30	2.49	4.30	4.66	4.95	5.40	5.90	6.80	7.10
$HfSe_2$	2.08	2.26	2.52	2.74	3.10	4.40*	4.75	5.10*	5.55	6.25	6.98	8.00

tra, which can be compared with the available band calculations.

In Fig. 3 a possible phenomenological correlation among TR structures for the compounds $TiSe_2$, $ZrSe_2$, and $HfSe_2$ as a function of the in-plane lattice parameter a is shown. The lattice parameters are taken from Table I. Circles indicate TR minima associated with interband transitions, while crosses mark TR structures associated with plasma resonances.

The representation of the energies of the structures taken from Figs. 4 and 5 as a function of the lattice parameter c, gives a roughly linear variation of the energy gap versus c for the sequences TiS_2-$TiSe_2$-$TiTe_2$; TiS_2-ZrS_2-HfS_2, and $TiSe_2$-$ZrSe_2$-$HfSe_2$. However, in the dependence of the gap energies on the lattice parameter a, only the sequence TiS_2-$TiSe_2$-$TiTe_2$ shows a linear variation. The remaining sequences behave as shown in Fig. 3. Note all the plots of such energies are reported here for brevity, since the general behavior is quite similar to those already published.[18,19] However we remark that our results, which are obtained at low temperature and by means of a derivative technique, allow one to measure directly and with a better resolution the position of the optical structures, some of which were determined through fitting procedures in previous works.[19] Thus, finer details in a wider energy range (1—9 eV instead of 1—4 eV) were obtained in the present work, confirming the general trends already shown in Ref. 19.

Theoretical curves of reflectivity, absorption coefficient, permittivity and energy loss have been obtained from a recent band calculation,[14] based on Hartree-Fock-Slater theory. A direct comparison of them with experimental spectra shows satisfactory agreement and gives for the main optical structures detailed information, summarized in Table II, where the optical features are denoted as A_i and B_i (see Table II) according to the Ref. 14.

In order to obtain more specific information about transitions at high-symmetry points of the Brillouin zone, the optical surface of the sample as well as light polarization should be considered, as it has been done below 4 eV.

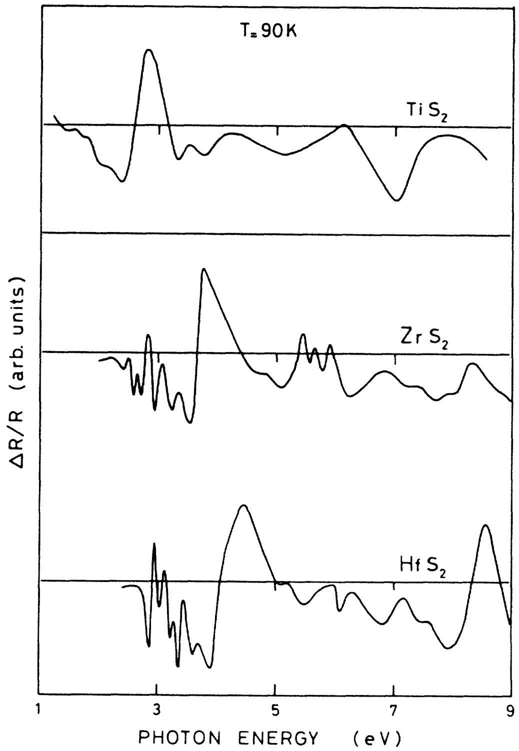

FIG. 4. Thermoreflectance spectra at 90 K for TiS_2, ZrS_2, and HfS_2 crystals.

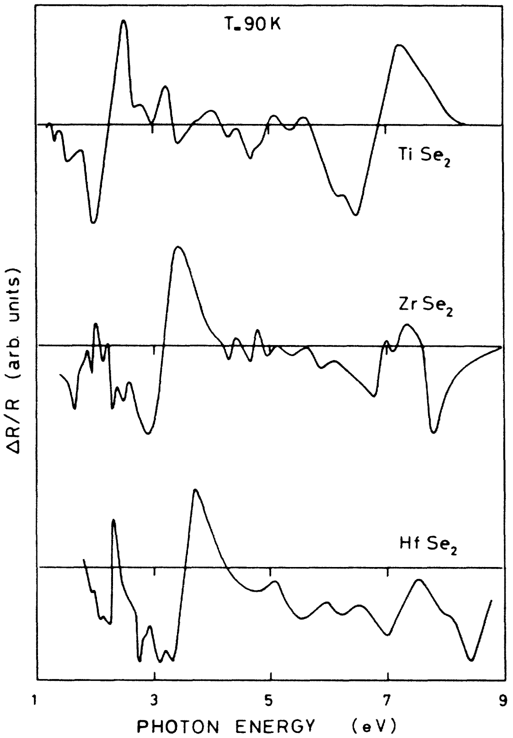

FIG. 5. Thermoreflectance spectra at 90 K for $TiSe_2$, $ZrSe_2$, and $HfSe_2$ crystals.

Such a study, however, was not undertaken in the present work, since the attention was focused on the general correspondence among the structures of the interband spectra. This point will be clarified in the next section.

IV. $Ti_{1-x}Hf_xSe_2$: A TRANSITION FROM SEMIMETALLIC TO SEMICONDUCTING STATE

The group-IV TMD's are generally semiconductors. They are semimetals only if the p valence band and the lowest d conduction band overlap. This is the case of $TiSe_2$, which is characterized by an overlap (negative energy gap) of -0.2 eV. On the contrary, $HfSe_2$ is a semiconductor with an indirect band gap of 1.13 eV. In the mixed system $Ti_{1-x}Hf_xSe_2$, the crossing of the valence and of the conduction band occurs for $x=0.3$.[24,25]

In this paper we intend to show a strict correlation between the evolution of the optical spectra and the variation of the structural parameters a, c, and z when the composition changes.

In this context a result of primary importance is that, up to the maximum value of x which can be reached ($x=0.5$), the unit cell does not show any appreciable distortion despite the larger size of the Hf atoms. The parameters a, c, and z (as well as the composition x), as reported in Fig. 6 and in Table III, were determined by x-ray structure measurements, showing that Hf atoms occupy substitutional positions. Note that, while a and c grow linearly as a function of x $(0 \leq x \leq 0.5)$ with a slope which within 1% gives the correct extrapolation to the values typical of $HfSe_2$ ($a=3.75$ Å, $c=6.16$ Å), z does remain constant.

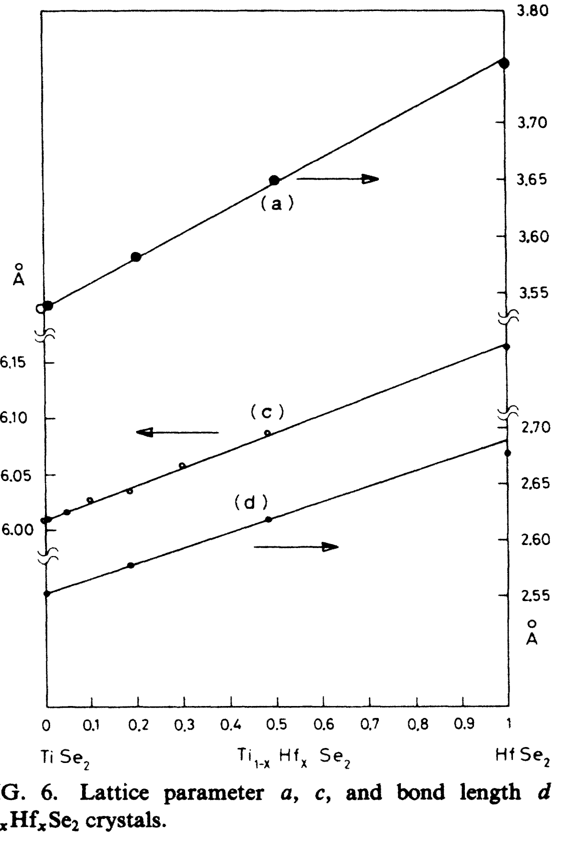

FIG. 6. Lattice parameter a, c, and bond length d for $Ti_{1-x}Hf_xSe_2$ crystals.

TABLE III. Lattice parameters a, c, Ti—Se bond length d, and structural parameter z at different composition for the crystals $Ti_{1-x}Hf_xSe_2$.

x	a (Å)	c (Å)	d (Å)	z
0.0	3.54	6.01	2.552	0.2547±0.0005
0.1	3.56	6.025	2.566	0.2549±0.0005
0.2	3.58	6.04	2.58	0.2549±0.0005
0.3	3.60	6.056	2.594	0.2550±0.0005
0.4	3.63	6.072	2.609	
0.5	3.65	6.087	2.623	0.2560±0.0005

On the basis of these results, a more complete and quantitative evaluation can now be made of the variation of the energy position of the structures due to interband transitions versus x. In addition to the results of the present investigation, TR spectra already published[20] have been reconsidered and are reported in Fig. 7. The compo-

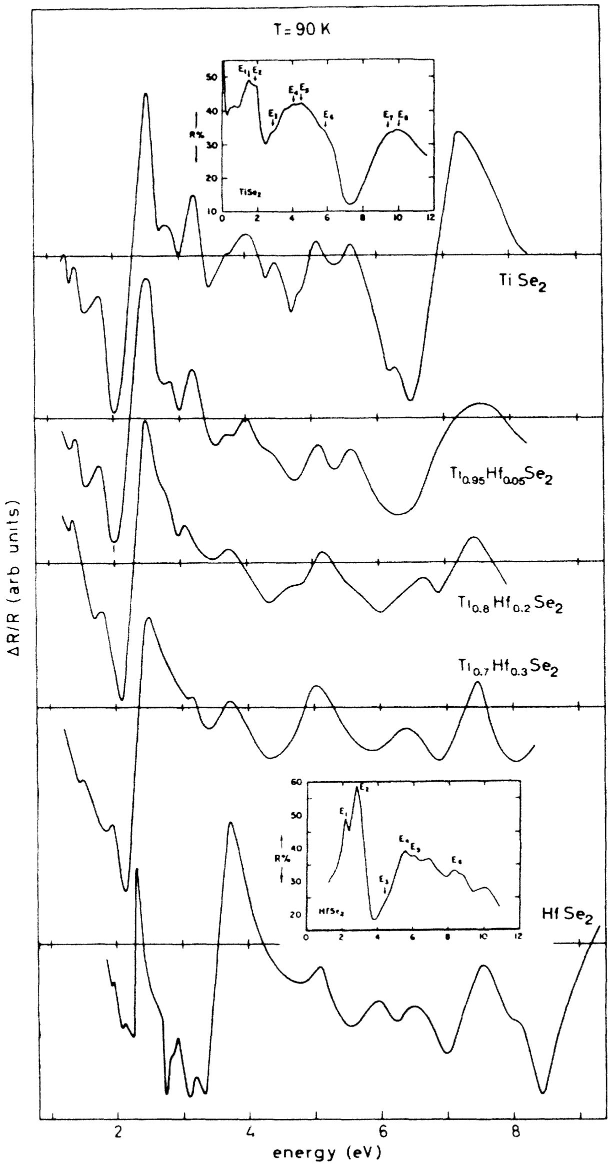

FIG. 7. Thermoreflectance spectra for $Ti_{1-x}Hf_xSe_2$ crystals. Insets showing reflectance spectra at room temperature are taken from Ref. 18.

sition dependence of the typical structure energies is reported in Fig. 8. The values of A_i and B_i do not follow at all the a and c variation in the mixed series, but they keep practically their constant value from $x=0$ to $x=0.5$, as the z parameter does. The large discrepancy (having maximum values of 0.3—0.4 eV) existing between the experimental slope in Fig. 8 for $Ti_{1-x}Hf_xSe_2$ crystal ($0 \leq x \leq 0.5$) and that pertaining to the concentration-weighted average of the constituent dichalcogenides $TiSe_2$ and $HfSe_2$ at a given composition, indicates that fundamental differences exist in the electronic states involved in bonding in $TiSe_2$ and $HfSe_2$. Due to the presence of Ti and Hf in the mixed crystals, the multiple scattering of electrons in the disordered arrangement of the two different transition metals is expected to influence the composition dependence of A_i and B_i.

Chemical disorder and bond-length variations have been shown to be effects of primary importance in semiconducting zincblende alloys.[26—28] In this connection, the atomic size mismatch parameter[27]

$$\delta=\frac{R_{ac}^2-R_{bc}^2}{R_{ac}^2+R_{bc}^2} \tag{3}$$

(where R_{ac} and R_{bc} are the Hf—Se and Ti—Se bond lengths) can be checked to be $\simeq 5$—6 %, which is comparable with the value of δ obtained for the $InGaAs_2$ alloy[27] ($\simeq 7\%$).

Similarly, the results illustrated in Fig. 8 suggest a bimodal distribution of bonds, which is also supported by the two-mode behavior of the phonon structures reported in Ref. 29.

At this point, note should be taken of Ref. 17, where z is given the role of the leading parameter in controlling the semimetal-semiconductor transition. Our results do not contradict the main conclusion of that work, since $A_i(x)$, $B_i(x)$, and $z(x)$ have a parallel behavior, although a thorough check of the model would require observing the evolution of A_i and B_i in a sufficiently wide range of the parameter z. From our data it appears that substantial variations of z through the substitution of Hf atoms in $TiSe_2$ crystals cannot be obtained. Other methods, based, e.g., on uniaxial stress or hydrostatic pressure application, may be much more effective in that respect.

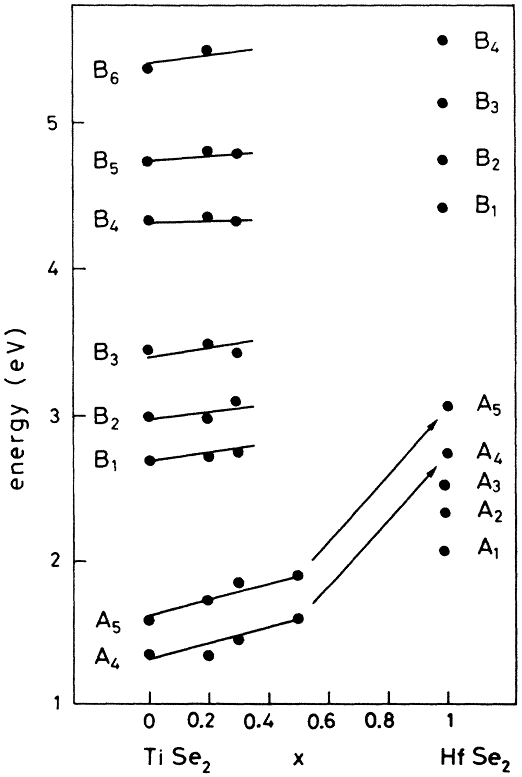

FIG. 8. Energies of optical structures in interband spectra versus composition for $Ti_{1-x}Hf_xSe_2$ crystals.

Finally, a last comment is to be made about plasmons at $\simeq 3$ and 7 eV in $Ti_{1-x}Hf_xSe_2$ mixed compounds. The faster disappearance as a function of composition of the plasmon at 7 eV (see Fig. 7) is the most striking result concerning this point. As for the "anomaly," one should stress the fact that an exhaustive calculation of the scattering of plasmons with respect to disordered periodicities is still lacking and intuitively no straightforward explanation can be found for the different behavior of the two plasmons at wavelengths $\lambda \gg a(x)$ and $\lambda \gg c(x)$. The smearing of the huge dispersionlike plasmon structure at $\simeq 7$ eV should be related to a more pronounced effect of disorder on the higher-energy plasmon or to a different effect of the gradual growth of the interband spectra of $HfSe_2$ in the two energy regions. General theoretical treatments are needed in order to get a clear understanding of this point.

V. CONCLUSIONS

The main conclusions of the work are here summarized.

(i) TR measurements at low temperature allow a direct determination of optical structures with high resolution in a wider energy range (1—9 eV) than in previous works.

(ii) The TR line shape is interpreted in terms of thermal broadening as the prevailing mechanism.

(iii) Anomalies in the interband spectra as a function of composition and structural parameters have been observed and studied. Such anomalies can be interpreted in terms of a bond alternation model (bimodal distribution).

(iv) As for the plasmons at 3 and 7 eV in $TiSe_2$, the faster disappearance of the latter one as a function of composition is briefly discussed and qualitatively explained in terms of sensitivity of the TR technique in giving indirect evidence of the initial growth of the interband spectra of $HfSe_2$ in the alloy for $x < 0.5$ or of the influence of disorder on the collective modes.

ACKNOWLEDGMENTS

The authors wish to thank Professor G. Rossi of Centro Studio per la Cristallografia Strutturale del Consiglio Nazionale delle Ricerche (Pavia, Italy) for performing the x-ray measurements. One of the authors (C.C) acknowledges support from the "International Center of Theoretical Physics of Trieste Programme for Training and Research." Some of the authors (A.B., G.G., L.N., E.R., and A.S.) are part of the Centro Interuniversitario di Struttura della Materia del Ministero della Pubblica Istruzione and the Gruppo Nazionale di Struttura della Materia del Consiglio Nazionale delle Ricerche, Italy.

[*] Permanent address: Physics Department, Peking University, Beijing, China.

[1] *Physics and Chemistry of Materials with Layered Structure,* edited by F. Lévy (Riedel, Dordrecht, 1976), Vols. 2 and 4.

[2] L. F. Mattheiss, Phys. Rev. B **8**, 3719 (1973).

[3] R. B. Murray, R. A. Bromley, and A. D. Yoffe, J. Phys. C **5**, 746 (1972).

[4] P. Krusius, J. von Boehm, and H. M. Isomaki, J. Phys. C **8**, 3788 (1975).

[5] H. M. Isomaki and J. von Boehm, Nuovo Cimento B **38**, 168 (1977).

[6] A. Zunger and A. J. Freeman, Phys. Rev. B **16**, 906 (1977).

[7] A. Zunger and A. J. Freeman, Phys. Rev. B **17**, 1839 (1978).

[8] D. W. Bullet, J. Phys. C **11**, 4501 (1978).

[9] H. M. Isomaki, J. von Boehm, and P. Krusius, J. Phys. C **12**, 3239 (1979).

[10] H. M. Isomaki and J. von Boehm, Phys. Lett. **89A**, 89 (1982).

[11] J. von Boehm and H. M. Isomaki, J. Phys. C **15**, L733 (1982).

[12] C. Umrigar, D. E. Ellis, Deng-sheng Wang, H. Krahauer, and M, Posternak, Phys. Rev. B **26**, 4935 (1982).

[13] J. von Boehm and H. M. Isomaki, Phys. Rev. B **26**, 5798 (1982).

[14] H. M. Isomaki and J. von Boehm, Phys. Rev. B **26**, 5807 (1982).

[15] R. Coehoorn, A. van Heuzen, C. Haas, G. A. Sawatzky, and R. A. de Groot, in the 5th General Conference on the Condensed Matter Division (West Berlin, 1985) (unpublished), Abstract, SCP 20.

[16] H. Suzuki, A. Yamamoto and K. Motizuki, Solid State Communication **49**, 1039 (1984).

[17] A. Zunger and A. J. Freeman, Phys. Rev. Lett. **40**, 1155 (1978).

[18] D. L. Greenaway and R. Nitsche, J. Phys. Chem. Solids **26**, 1445 (1965).

[19] S. C. Bayliss and W. Y. Liang, J. Phys. C **15**, 1283 (1982).

[20] A. Borghesi, G. Guizzetti, L. Nosenzo, E. Reguzzoni, A. Stella, and F. Lévy, Nuovo Cimento **D4**, 141 (1984).

[21] B. Batz, in *Semiconductors and Semimetals,* edited by R. K. Willardson and A. C. Beer (Academic, New York, 1972), Vol. 9.

[22] M. G. Bell and W. Y. Liang, Adv. Phys. **25**, 53 (1976).

[23] A. Couget, L. Martin and F. Pradal, C. R. Acad. Sci. B **272**, 626 (1971).

[24] I. Taguchi, J. Phys. C **14**, 3221 (1981).

[25] A. Borghesi, M. Geddo, G. Guizzetti, E. Reguzzoni, A. Stella, and F. Lévy, Phys. Rev. B **29**, 3167 (1984).

[26] J. C. Mikkelsen, Jr. and J. B. Boyce, Phys. Rev. Lett. **49**, 1412, (1982).

[27] A. Zunger and J. E. Jaffe, Phys. Rev. Lett. **51**, 662 (1983).

[28] R. C. Hass, R. J. Lempert, and H. Ehrenreich, Phys. Rev. Lett. **52**, 77 (1984).

[29] I. Taguchi, H. P. Vaterlaus, and F. Lévy, Solid State Commun. **49**, 79 (1984).